medRxiv preprint doi: https://doi.org/10.1101/2020.04.24.20078576; this version posted May 1, 2020. The copyright holder for this preprint (which was not certified by peer review) is the author/funder, who has granted medRxiv a license to display the preprint in perpetuity. It is made available under a CC-BY-NC-ND 4.0 International license .

Modeling serological testing to inform relaxation of social distancing for COVID-19 control

Alicia N. M. Kraay*[,1], Kristin N. Nelson*[,1], Conan Zhao[2,3], Joshua S. Weitz[2,4,5], Benjamin A. Lopman[1]

[1] Rollins School of Public Health, Emory University, Atlanta, GA, USA
[2] School of Biological Sciences, Georgia Institute of Technology, Atlanta, GA, USA
[3] Interdisciplinary Graduate Program in Quantitative Biosciences, Georgia Institute of Technology, Atlanta, GA, USA
[4] School of Physics, Georgia Institute of Technology, Atlanta, GA, USA
[5] Center for Microbial Dynamics and Infection, Georgia Institute of Technology, Atlanta, GA, USA

April 24, 2020

Abstract

Background: While social distancing efforts have been successful at slowing the spread of SARS-CoV-2, these measures cannot be sustained indefinitely. In this paper, we examine how serological testing can reduce the risk of relaxing social distancing measures while also providing a way for test-positive individuals to return to more normal levels of activity.

Methods: We use an SEIR-like compartmental model that accounts for serological test status to examine if widespread serological testing can reduce the adverse effects of relaxing social distancing measures, in terms of total deaths and health system burden. In our model, social distancing measures are relaxed to a greater extent for those who test positive compared to those who have not been tested or test negative, allowing a return to work and partial restoration of other social contacts to pre-pandemic levels. All individuals preferentially interact with those who have tested positive, such that seropositive individuals act as immunological 'shields.' We consider a range of potential testing capacities and the implications of an imperfect test for this strategy.

Results: Although relaxing social distancing interventions increases total deaths, serologic testing as a part of this strategy can reduce population risk. If social distancing restrictions are relaxed by 50% in tandem with monthly serological testing of the general United States (US) population, 174,000 deaths would be averted and 67% of the US population would be released from social distancing after 1 year, as compared to a scenario without serological testing. Sustaining moderate levels of social distancing can help to flatten the epidemic curve, reducing health system burden below the US critical care capacity.

Implications: Modeling studies suggest that serological testing can be used to relax social distancing measures preferentially for seropositive individuals, insofar as antibodies can be established as a correlate

*These authors contributed equally to this work

NOTE: This preprint reports new research that has not been certified by peer review and should not be used to guide clinical practice.

medRxiv preprint doi: https://doi.org/10.1101/2020.04.24.20078576; this version posted May 1, 2020. The copyright holder for this preprint (which was not certified by peer review) is the author/funder, who has granted medRxiv a license to display the preprint in perpetuity. It is made available under a CC-BY-NC-ND 4.0 International license .

of protection against SARS-CoV-2 infection. Implementing a strategy of serological testing and shielding can reduce population risk while offsetting the severe social and economic costs of a sustained shutdown.

1 Introduction

SARS-CoV-2 emerged in central China in late 2019 leading to an ongoing pandemic of COVID-19, with over 2.5 million detected cases and over 175,000 deaths globally as of April 23, 2020 [1]. In the United States, 600,000 cases and 25,000 deaths were reported by that date [1]. Unprecedented 'social' or 'physical' distancing measures have been put in place to reduce transmission and thereby blunt the epidemic peak (i.e. "flatten the curve"). Beginning early in March, U.S. states began to close schools, suspend public gatherings, and encourage employees to work from home if possible. On March 17, 2020, the US federal government issued national social distancing guidelines, leading to wider implementation of such policies throughout the country. At present, 95% of the U.S. [2] and over 30% of the global population is under some form of lockdown or government-issued shelter-in-place order [3]. However, the U.S. federal guidelines are set to expire on April 30, 2020, which may result in some activities resuming and facilities re-opening in a matter of weeks [4].

While initial data suggests that early social distancing guidelines may have initially helped slow the spread of COVID-19 in many countries, including the United States, relaxation of social distancing will result in increased contacts and therefore transmission increasing once again in the community. A return to 'business as usual' without any restrictions would see a return to exponential growth in cases, rapidly exceeding the capacity of health services [5].

With the goal of maintaining the reproductive number at or less than one, strategic public health efforts could allow a gradual return to some activities [4]. Some degree of social distancing is likely to be maintained, whereby people have fewer (potentially infectious) contacts. Strict distancing measures can remain in place for individuals at higher risk including the elderly and people with underlying health conditions. However, widespread serological testing programs may be useful to inform social distancing recommendations in the next phase of the U.S. epidemic.

Although rigorous population-based serosurveys of SARS-CoV2 in the United States have yet to yield results, it is highly likely that infections far outnumber documented cases [6]. To the extent that detectable antibodies serve as a correlate of immunity, serological testing may be used to identify protected individuals [7]. Germany, for example, has plans to test millions of people and to provide 'immunity passports' to those who test positive [8]. Moreover, it has been proposed that immune individuals could be returned to society in a more efficient way by having them act as 'shields' [9]. In this strategy, shields would preferentially replace susceptible individuals in physical interactions, such that more contacts are between susceptible and recovered (immune) individuals rather than between susceptible and potentially infectious individuals.

Such strategies, however, rely on a serological test that can correctly identify immune individuals. At the moment a small number of serological assays for detection of SARS-CoV-2 antibodies have been approved for emergency use by Food and Drug Administration (FDA) [10] with many others currently in development (e.g. [11]). These tests and likely others that become available will be imperfect[12, 13]. For the purpose of informing social distancing, specificity (rather than sensitivity) is of primary concern. An imperfect test will inevitably lead to false positive results, which in this context leads to individuals being incorrectly classified

medRxiv preprint doi: https://doi.org/10.1101/2020.04.24.20078576; this version posted May 1, 2020. The copyright holder for this preprint (which was not certified by peer review) is the author/funder, who has granted medRxiv a license to display the preprint in perpetuity. It is made available under a CC-BY-NC-ND 4.0 International license .

as immune. If used as a basis to relax social distancing measures, this error could lead to an increase in transmission. The probability that a person with a positive test truly has immunity (the positive predictive value) will change over the course of the epidemic as true prevalence increases.

Here, we evaluate the epidemiological consequences of using mass serological testing to inform the relaxation of social distancing measures as the COVID-19 epidemic progresses.

2 Methods

2.1 Model structure

We modeled the transmission dynamics of SARS-CoV-2 using a deterministic, compartmental SEIR-like model. (Figure 1) We assume that after a latent period, infected individuals progress to either undocumented or documented infection. A fraction of symptomatic cases are severe enough to seek care and become documented infections. A proportion of those with documented infection are hospitalized, with a subset of those requiring critical care. Surviving cases, both undocumented or documented, recover and are assumed to be immune to reinfection (Table 1). All individuals who have not tested positive and are not currently experiencing symptoms of respiratory illness are eligible to be tested. All hospitalized cases are tested prior to discharge. Recovered individuals are moved to the test positive group at a rate that is a function of the test sensitivity. Susceptible, latently infected, and undocumented cases may falsely test positive and are moved to the test positive group at a rate that is a function of test specificity. False positives may become infected, but the inaccuracy of their test result is not recognized unless they develop symptoms that are sufficiently severe to warrant hospitalization and health providers correctly diagnose COVID-19, overriding the history of a positive antibody test. The ordinary differential equations corresponding to this model are included in the supplemental material. All models were run using R in the package 'deSolve' in R version 3.6.2. Code is available at `https://github.com/lopmanlab/Serological_Shielding`.

There are three age groups represented in the model: children and young adults (<20 years), working adults (20-64 years), and elderly (65+ years). We modeled age-specific mixing based on POLYMOD data adapted to the population structure in the United States [14, 15]. Contacts in this survey were reported based on whether they occurred at home, school, work, or another location. We model an outbreak that begins with the first cases in the U.S., which were estimated to have occurred in mid-January [16, 17]. We assume the U.S. outbreak began on January 15, which we seed with 171 infections (60 in children, 71 in adults, and 40 in the elderly; initial conditions were calibrated to the initial time course of the outbreak).

2.2 Interventions

2.2.1 Social Distancing

On March 17, the U.S. federal government released guidance recommending working from home, postponing unnecessary travel, and limiting gatherings to less than 10 people [18]. Some states and municipalities issued their own guidance before this date, others after. To account for variations in timing, we assumed that national social distancing began on March 25th. Although adherence to these measures varies geographically and is generally difficult to measure, we made several assumptions about how these policies have changed location-specific contacts. First, we assume that under these measures, all contacts at school and daycare

medRxiv preprint doi: https://doi.org/10.1101/2020.04.24.20078576; this version posted May 1, 2020. The copyright holder for this preprint (which was not certified by peer review) is the author/funder, who has granted medRxiv a license to display the preprint in perpetuity. It is made available under a CC-BY-NC-ND 4.0 International license .

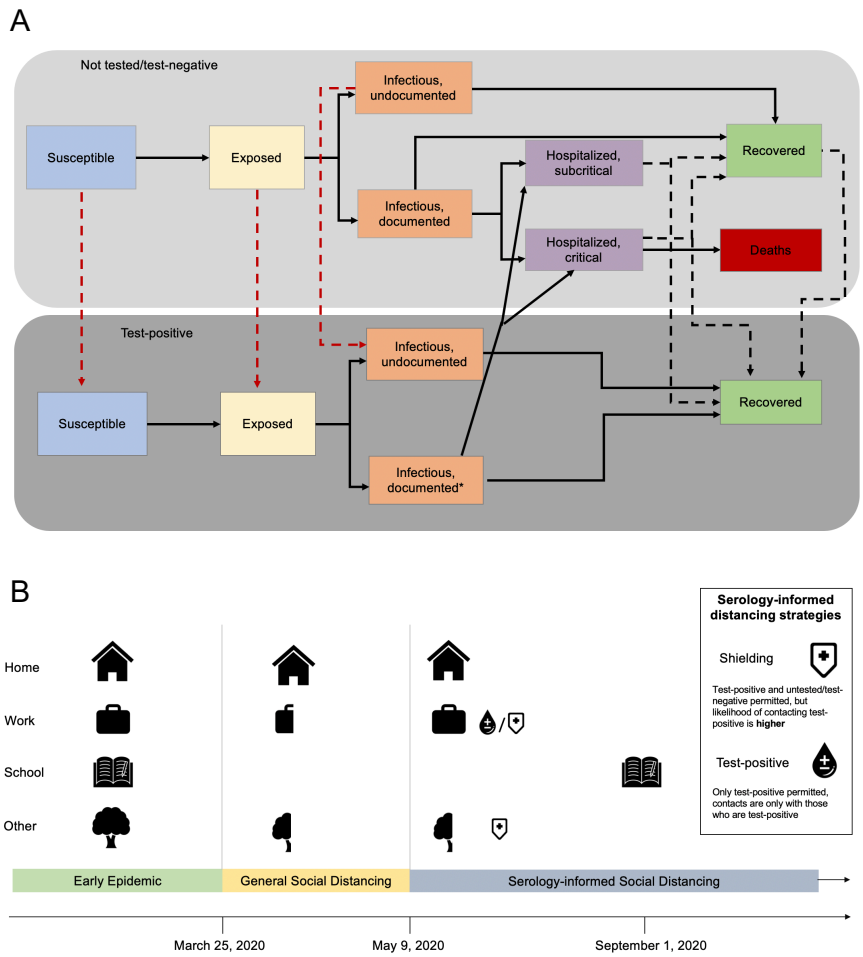

Figure 1: A) Overall model diagram. Serological antibody testing is shown by dashed arrows. Red dashed arrows indicate false positives (i.e., someone is not immune, but they are moved to the test positive group) and occur at a rate that is a function of 1-specificity. True positives occur at a rate that is a function of the sensitivity. *Documented infections in the test-positive group have similar severity to documented infections in the not tested/test negative group, but symptoms may not be recognized as being caused by SARS-CoV-2 unless symptoms are severe enough to warrant hospitalization. B) Schematic of modeled interventions. General social distancing reduces work, school and other contacts beginning on March 25, 2020 and these contacts are gradually reintroduced beginning on May 9, 2020 with schools and daycares re-opening on September 1, 2020.

medRxiv preprint doi: https://doi.org/10.1101/2020.04.24.20078576; this version posted May 1, 2020. The copyright holder for this preprint (which was not certified by peer review) is the author/funder, who has granted medRxiv a license to display the preprint in perpetuity. It is made available under a CC-BY-NC-ND 4.0 International license .

were eliminated and that contacts at non-home, non-work, non-school ('other') locations were reduced by 75%. We assume that contacts at home remain unchanged. To address differences in work-based contacts by occupation type, we classified the working adult population into three subgroups based on occupation: those with occupations that enable them to work exclusively from home during social distancing, those continuing to work but reduced their contacts at work by 90% (e.g., customer-facing occupations such as retail), and those continuing to work with no change in their contact patterns (e.g., frontline healthcare workers). The percent reduction in other contacts, percent contact reductions for essential workers who can reduce their contacts, and the timing of the start of national social distancing were calibrated by fitting to incidence observed in the US under social distancing such that the estimated number of deaths was within an order of magnitude to that reported on April 16, 2020. This corresponds to a 64.7% reduction in overall contacts for working-age adults, which is consistent with initial data from reductions in face to face contacts, which ranged from 50-85% [19].

2.2.2 Phased re-opening

Overall. We consider a phased approach to re-opening that begins to relax social distancing restrictions on May 1, 2020 and that these changes begin to affect contact patterns one week later on May 9, 2020. At this time, we assume that schools and daycares remain closed but that social distancing measures for the general population can be relaxed, by allowing work and other contacts to be increased. To represent this, we scale 'work' and 'other' contacts to a proportion of their value under general social distancing based on a scalar constant, c, such that $c = 1$ is equivalent to the scenario in which social distancing measures as put into place on March 17 are maintained and $c = 0$ is equivalent to a return to pre-pandemic contact levels for both 'work' and 'other' contacts for essential workers and pre-pandemic contact levels for "other contacts for all other groups. We assume that all children return to school and daycare on September 1,2020.

Testing. We consider how complementing relaxation of social distancing with serological testing could be used to both release test-positive individuals from social distancing to act as shields, reducing population risk. We assume that testing begins on May 1, 2020, and that test results begin to affect contact patterns one week later on May 9, 2020.

Individuals that test positive can return to work (if they are not already working) and can increase their non-home and non-school contacts to normal levels. To represent the deployment of immune persons in customer-facing and other high-contact occupations, we assume that contacts at work and other (non-home, non-school) locations are preferentially with immune persons by specifying that the probability of interacting with a test positive person is 5 times what would be expected given the frequency of test-positives in the population (α=4), modeled using 'fixed shielding' as described previously in [9]. We consider alternative α values in a sensitivity analysis.

For our primary models, we assume a serological test with a sensitivity of 94% and a specificity of 96%, consistent with the reported accuracy of FDA-approved tests currently in use [10] (alternative assumptions are explored in sensitivity analysis). We consider how relaxing social distancing recommendations combined with different levels of serological testing (daily tests performed ranging from 0 to 10 million) impacts the proportion of the population released from social distancing, total deaths, and peak health system burden.

medRxiv preprint doi: https://doi.org/10.1101/2020.04.24.20078576; this version posted May 1, 2020. The copyright holder for this preprint (which was not certified by peer review) is the author/funder, who has granted medRxiv a license to display the preprint in perpetuity. It is made available under a CC-BY-NC-ND 4.0 International license .

3 Results

3.1 No testing

In the absence of any intervention, our model predicts that 85% of the US population would be infected with SARS-CoV-2, resulting in a total of 1.1 million deaths. Social distancing has the potential to greatly reduce this burden, with indefinite social distancing reducing cumulative deaths by 83% and leading to a flattened epidemic curve. However, if social distancing measures are relaxed prematurely, incidence rebounds quickly and the benefit of early distancing is lost by the end of the epidemic (see SI).

3.2 Testing-informed social distancing

While relaxing social distancing leads to increases in deaths, reductions in social distancing may be implemented simultaneously with serological testing to reduce deaths and strain on the healthcare system (Figure 2, Figure 3). We estimate that current social distancing policies have reduced total contacts for adults by 65%, which is supported by recent estimates [19]. If social distancing measures are relaxed such that adults only reduce their contacts by 41% compared with pre-pandemic levels (c=0.5) and schools are reopened in the fall, 688,000 deaths would be expected by January 15, 2021 (Figure 2). However, if yearly serological testing of the US population (1 million tests/day) is also implemented in tandem with nationwide relaxation of social distancing, expected deaths fall to 561,000, saving 127,000 lives. If monthly testing is achievable (10 million test/day), expected deaths fall to 514,000, saving an additional 47,000 lives. In the same scenario with monthly testing, 67% of the US population would test positive by the end of one year and be able to both return to work and increase other social contacts to pre-pandemic levels (Figure 3, 24% if yearly testing is used). The magnitude of this benefit depends on the degree of immunological shielding–if $\alpha = 0$ (no shielding), 726,000 deaths would be expected, more than if testing were not implemented at all. In other words, testing can adversely affect population risk if not accompanied by changes in interactions. Higher levels of shielding did not appreciably impact population risk (see SI).

While the fraction of the test positive population who is truly immune depends on both social distancing levels and testing rate, roughly 30% of the test positive population would remain susceptible at the end of the epidemic if monthly testing of the US population were implemented (e.g., 30% of the test positive population would be false positives, see SI). Testing 200,000 people per day is roughly equivalent to a 10% increase in social distancing intensity (Figure 4). At higher levels of testing, these effects are more complex: one million tests per day reduces mortality equivalent to 50% increase in social distancing intensity for scenarios with weak social distancing, but can have perverse effects with very strong social distancing, if infection prevalence remains low and thus the rate of false positives is higher (Figure 3). While a test with 100% specificity would eliminate the potential for false positives, the impact of this change on cumulative deaths would be minimal.

For all scenarios, sustaining moderate levels of social distancing for test-negative and untested individuals is important to help reduce peak epidemic burden (Figure 3). Removing all restrictions on non-home and non-school interactions would result in a peak burden of 200,000 to 400,000 critical care patients in late June. In contrast, if social distancing measures remain relatively strong (c=0.75, equivalent to total contacts reduced by 53% for adults), peak burden would be 64,000-80,000 critical care patients, which is less than the current critical care capacity in the United States (estimated at 97,776 beds [20]).

medRxiv preprint doi: https://doi.org/10.1101/2020.04.24.20078576; this version posted May 1, 2020. The copyright holder for this preprint (which was not certified by peer review) is the author/funder, who has granted medRxiv a license to display the preprint in perpetuity. It is made available under a CC-BY-NC-ND 4.0 International license .

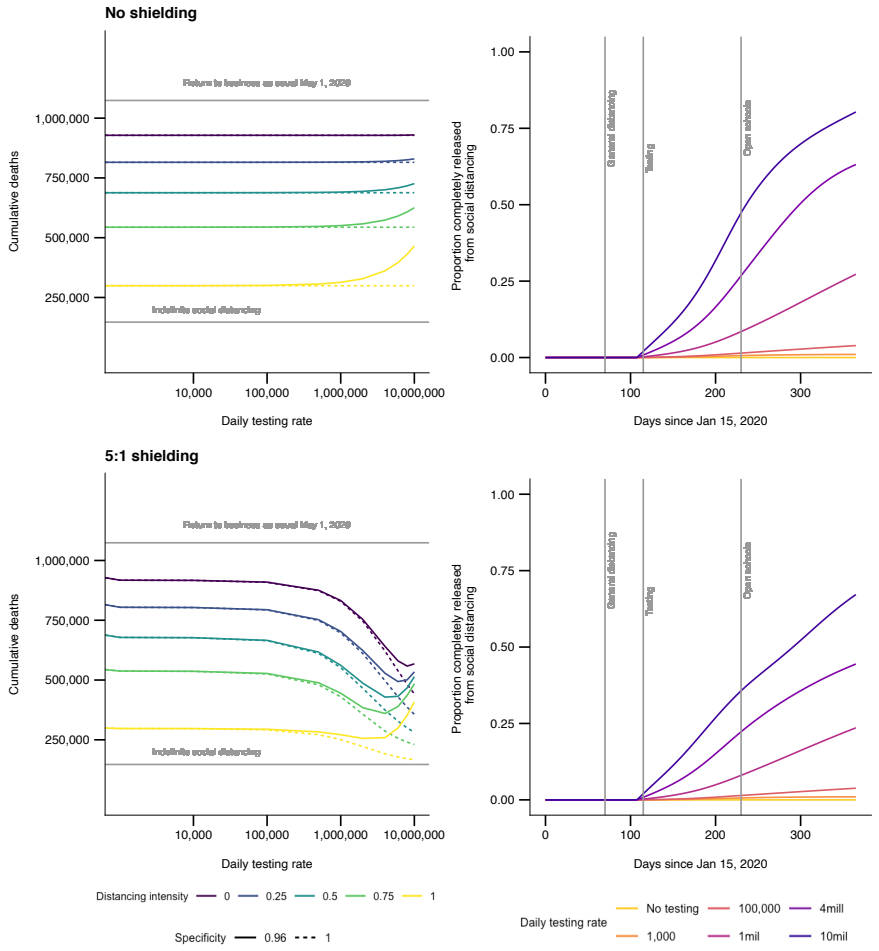

Figure 2: The left column shows cumulative deaths by January 15, 2021 by social distancing relaxing strategy assuming schools reopen on September 1, 2020 for No Shielding ($\alpha = 0$) (top) and 5:1 Shielding (bottom). Colored lines show levels of relaxing social distancing measures based on the value of c. Solid lines are for 96% specificity and dashed lines show results for a test with 100% specificity. The right column shows the fraction of the US population released from social distancing after 1 year for No Shielding (top) and 5:1 Shielding (bottom). Line colors correspond to testing levels, with blue being 10 million tests/day (monthly testing of the US population). All panels show a 50% relaxation of current social distancing levels for work and other contacts for those untested or testing negative and assume a test specificity of 96%.

medRxiv preprint doi: https://doi.org/10.1101/2020.04.24.20078576; this version posted May 1, 2020. The copyright holder for this preprint (which was not certified by peer review) is the author/funder, who has granted medRxiv a license to display the preprint in perpetuity. It is made available under a CC-BY-NC-ND 4.0 International license .

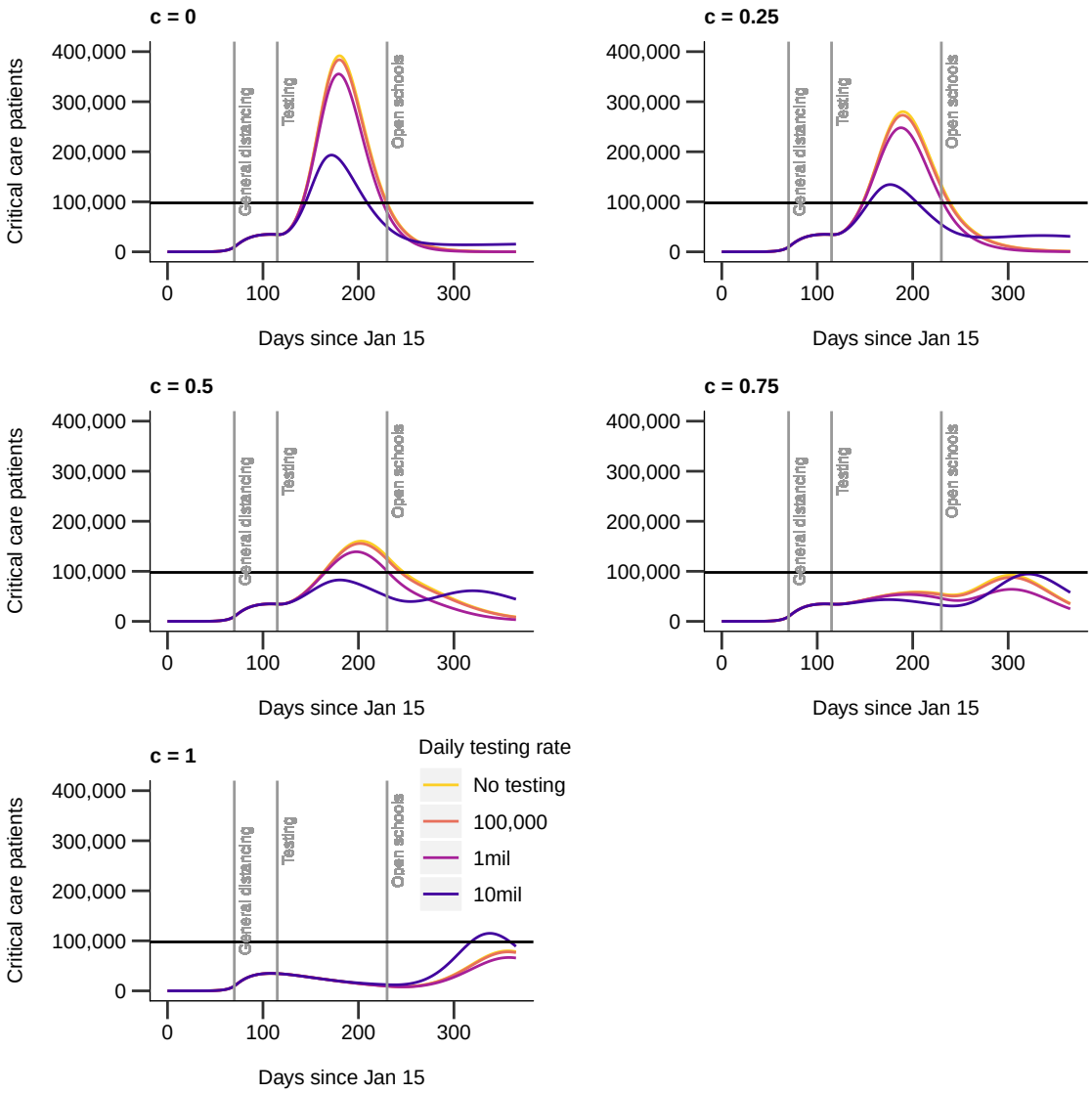

Figure 3: Critical care cases over time by testing level (colors) and relaxation of social distancing levels for other contacts and workplace restrictions (panels). c is the factor by which non-home, non-school contacts are reduced from their initial values. All panels assume schools reopen on September 1, 2020. The 'No testing' scenario is shown in yellow and is nearly identical to the 100,000 tests per day scenarios. The US critical capacity is shown by the solid black line (97,776 beds)

medRxiv preprint doi: https://doi.org/10.1101/2020.04.24.20078576; this version posted May 1, 2020. The copyright holder for this preprint (which was not certified by peer review) is the author/funder, who has granted medRxiv a license to display the preprint in perpetuity. It is made available under a CC-BY-NC-ND 4.0 International license .

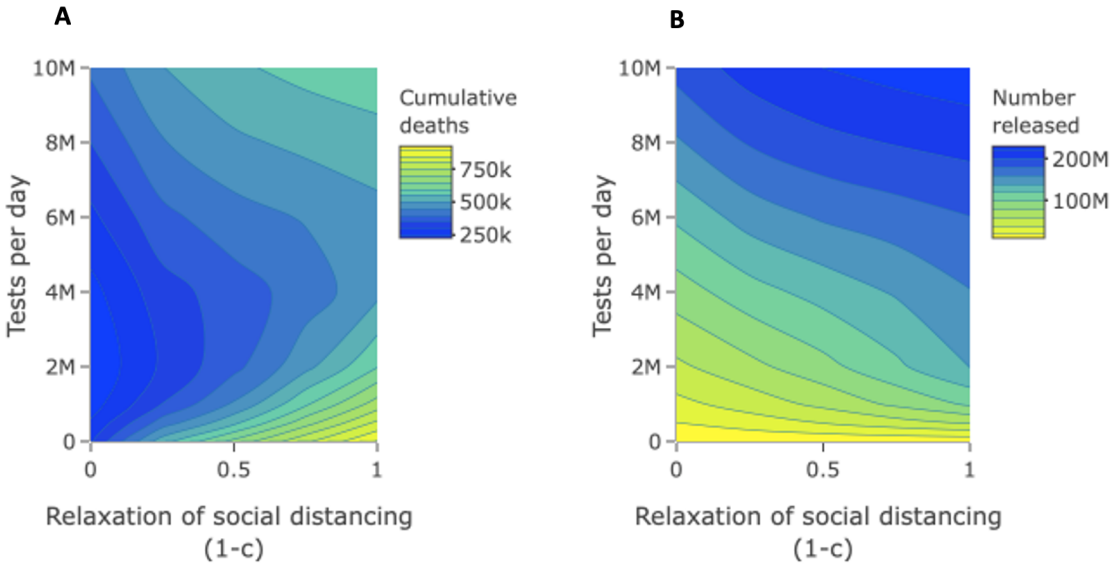

Figure 4: Contour plot of A) cumulative deaths and B) number of people released from social distancing as a function of the degree of relaxation of social distancing $(1 - c)$ and number of tests per day. Both panels assume a test specificity of 0.96 and a shielding factor of 5:1 ($\alpha = 4$).

School reopening in early fall is unlikely to trigger a second wave of infections unless the US remains under nationwide lockdown until the start of the academic year ($c = 1$). A secondary peak is more likely to occur during the summer, after social distancing measures are initially relaxed. If the US elects to maintain social distancing at its current level until early fall, small increases in transmission may occur after schools reopen. Note that our model does not account for any seasonal variation in transmissibility, which may or may not be an important factor for SARS-CoV-2 transmission [21].

4 Discussion

There is an urgent need to identify strategies that will permit safely easing lockdown measures and returning to productive levels of economic and social activity. Our models suggest that serological testing can make an important contribution to these efforts. Maintaining a moderate level of social distancing (i.e., at half the current level) together with an aggressive serological testing program (at least yearly testing) could release 24 to 67% of the population from social distancing within the first year of the COVID-19 pandemic. Individuals who test positive could act as 'shields' to reduce transmission, leading to greater reductions in overall deaths [9]. Although our model with moderate relaxation of social distancing plus monthly serological testing still results in 514,000 deaths, it also results in a flattened curve that provides time to improve treatment and expand healthcare capacity, which could ultimately reduce mortality rates [22]. Moreover, our models suggest that an approach with serological testing results in up to 174,000 fewer deaths than a strategy without testing, with promise of greater benefit if testing is targeted towards higher-risk groups [9]. In addition to fewer deaths, serological testing would also allow a substantial fraction of the population to return to work and other activities with relative safety, compared to a universal rollback of social distancing policies that would erase hard-earned gains we have made to date in controlling the spread of SARS-CoV-2 (see SI). Of course, a serological testing strategy is only one component of the response, alongside rigorous

medRxiv preprint doi: https://doi.org/10.1101/2020.04.24.20078576; this version posted May 1, 2020. The copyright holder for this preprint (which was not certified by peer review) is the author/funder, who has granted medRxiv a license to display the preprint in perpetuity. It is made available under a CC-BY-NC-ND 4.0 International license .

contact tracing efforts as incidence declines and sufficient capacity for diagnostic testing.

Although we do not consider the logistical challenges of mass serological testing initiative, we posit that this approach is feasible. Germany has already implemented serological testing on a large scale, including repeat testing of the same individuals on a regular (i.e. monthly) basis [23]. Although this would require a significant and rapid scale-up in testing capacity, significant scale-up has already been achieved for diagnostic PCR testing: from fewer than 1,000 tests per day in early March to nearly 150,000 tests per day in early April. Drawing whole blood samples requires trained healthcare personnel, which would likely be prohibitive in terms of cost and time on a mass scale. However, self-administered dried blood spot tests, which require only a finger prick, may address some of the logistical challenges of a mass serological testing program if assays can be optimized and validated for use on dried blood spots. Even if testing can be scaled up, requiring evidence of a positive test to return to work creates strong incentives for people to either misrepresent their immune status or intentionally get infected. A successful mass testing program must consider how a program would enforce existing social disparities and guard against potential inequities in the availability of testing. Moreover, a history of a positive antibody test should not change the clinical care of individuals with respiratory symptoms suggestive of SARS-CoV-2 infection if a PCR diagnostic test would otherwise be indicated.

Our models assumed random allocation of serological testing. In practice, testing targeted to specific groups, such as healthcare workers, food service employees, or people who suspect themselves to have been infected would increase efficiency by improving the positive predictive value of the test. Healthcare workers are likely to be first to be offered antibody testing. [11] This approach would likely increase the test positive rate, increasing cost-effectiveness [24]. In addition, the model of shield immunity that forms the basis for this analysis also showed how targeted use of shields to protect at-risk individuals can lead to substantive decreases in total hospitalizations and deaths [9].

While others have raised concerns that using an imperfect test to release social distancing pressures could increase population risk, we show here that even an imperfect diagnostic has utility because the prevalence of immune individuals is always greater in the test positive population than in the general population. Thus, deploying immune individuals so they are responsible for more interactions than susceptible individuals will always tend to decrease risk. If shielding is not used, this benefit disappears and testing can become a liability, which may explain why our findings differ from others [25]. In our model, cumulative deaths are not substantially impacted by the false positive rate given that deaths are similar when specificity is 100%. Although false positives are more important than false negatives for disease transmission risk, sub-optimal sensitivity also has implications for a mass testing strategy. The first FDA-authorized serological test has 94% sensitivity, which may reduce cost-effectiveness of testing by missing truly immune individuals. Complementing serology with PCR-based viral diagnostic testing could substantially increase the pool of immune people able to return to work and other activities. Strategies that use both tests should be the subject of future modeling studies.

Compared to maintaining current levels of lockdown, reducing social distancing always results in higher COVID-19 incidence. However, policymakers and society-at-large may consider these trade-offs acceptable, given the high social and economic costs of sustained social distancing. We show that complementing reductions in social distancing with the use of an imperfect diagnostic can offset this increased incidence, such that fewer deaths are expected if testing is used than if social distancing were implemented without testing. This benefit depends on deploying test positive individuals as shields. We have assumed a moderate degree of

medRxiv preprint doi: https://doi.org/10.1101/2020.04.24.20078576; this version posted May 1, 2020. The copyright holder for this preprint (which was not certified by peer review) is the author/funder, who has granted medRxiv a license to display the preprint in perpetuity. It is made available under a CC-BY-NC-ND 4.0 International license .

shielding [9], whereby people preferentially interact with presumed immune individuals (i.e. test positives). While this seems reasonable, the degree of preferential mixing assumed in our models is not informed by empirical data and the extent to which it is possible to implement this in different settings will vary. Critically, our model also incorporates realistic social contact patterns that account for contact differences and assortativity by age, occupation, and test status. The effect of relaxing social distancing measured, and the benefit of shielding, are likely sensitive to the nuanced changes in contact patterns by age, type, and location which are captured in model.

There remains much to learn about immunity to SARS-CoV-2 and we have made three critical simplifying assumptions in our model. First, we assume that antibodies are immediately detectable after resolution of infection. In reality, this likely occurs between 11 to 14 days post infection [26], similar to SARS-CoV-1 [27]. In practice, a small fraction of recent infections would be missed by serology, which would have a minor effect on our results. Second, we assume that immunity lasts for at least a year. Given that the virus has only been circulating for a matter of months in the human population, both the duration of antibody protection and the extent to which those antibodies protect against future infections is unknowable. Antibody kinetics of SARS-CoV-1 and MERS suggest that protection will last for at least months and as long as several years [27]. Ongoing studies of SARS-CoV-2 show that antibodies persist for at least 7 weeks, with more data to become available over the coming months [26]. Third, we assume that antibodies detected by serology are a correlate of protection. However, for some coronaviruses, antibodies do not appear to protect against subsequent infections[27]. To explore how this might impact our results, we conducted a sensitivity analysis where specificity was set to 50%, which assumes no discrimination between true and false positives. In this scenario, higher testing rates led to increased deaths due to increasing interactions with seropositive individuals with low levels of immunity (see SI). This increase in deaths was not apparent until testing rates reached 100,000/day, the same level at which a more specific test would be expected to begin to provide population level benefits.

In conclusion, our results suggest a role for a serological testing program in the public health response to COVID-19, given that the antibodies detected by such tests are established as a correlate of protection against infection. While maintaining a degree of social distancing, serology can be used to allow people with positive test results to return to work and other activities. Under most of our modeled scenarios, this approach served to release a sizable fraction of the population from social distancing, and, if those people serve as shields, to also reduce incidence of COVID-19.

Funding

BAL and ANMK were supported by the Vaccine Impact Modeling Consortium; BAL and KNN were supported by NIH/NICHD R01 HD097175; BAL, KNN, and ANMK were supported by NIH/NIGMS R01 GM124280; JSW and CZ were supported by Simons Foundation (SCOPE Award ID 329108); JSW and CZ were supported by the Army Research Office (W911NF1910384); JSW and CZ were supported by NIH (1R01AI46592-01); JSW and CZ were supported by National Science Foundation (1806606 and 1829636).

medRxiv preprint doi: https://doi.org/10.1101/2020.04.24.20078576; this version posted May 1, 2020. The copyright holder for this preprint (which was not certified by peer review) is the author/funder, who has granted medRxiv a license to display the preprint in perpetuity. It is made available under a CC-BY-NC-ND 4.0 International license .

Supplementary Material

S1. Social distancing interventions

If social distancing were completely relaxed prior to the end of the epidemic, our model predicts that transmission would quickly rebound. Predicted critical care epidemic curves are shown in Figure S1 and cumulative infections and deaths are shown in Table S1.

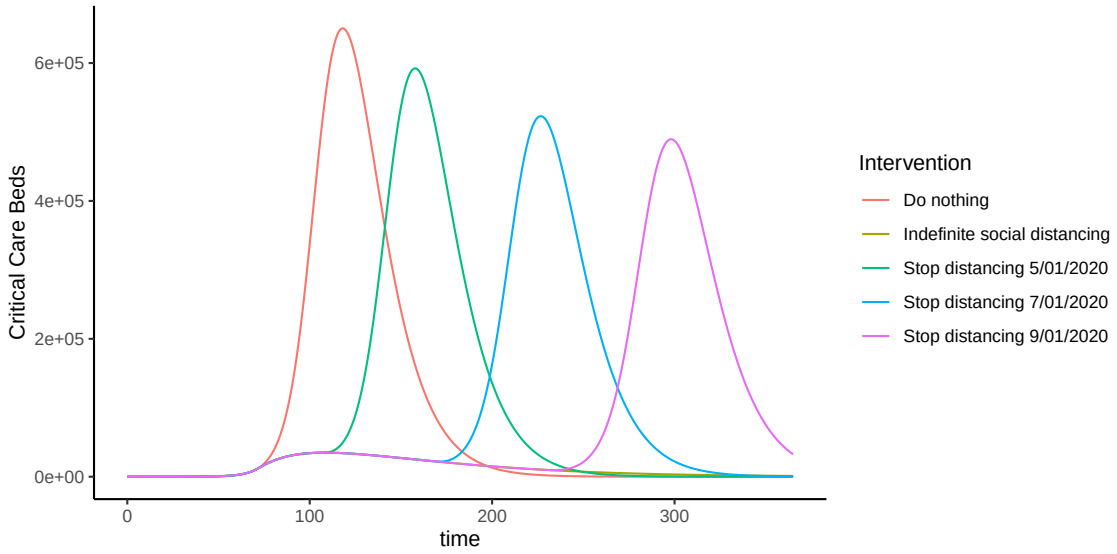

Figure S1: Critical care beds needed per day for different intervention scenarios assuming a 75% reduction in other contacts, school closures, nonessential workplace closures, and 90% reduction in workplace contacts for reduced contact employees for the duration of distancing

medRxiv preprint doi: https://doi.org/10.1101/2020.04.24.20078576; this version posted May 1, 2020. The copyright holder for this preprint (which was not certified by peer review) is the author/funder, who has granted medRxiv a license to display the preprint in perpetuity. It is made available under a CC-BY-NC-ND 4.0 International license .

Intervention	Cumulative infections (% US Population)	Deaths
Baseline		
Do nothing	272 mill (84.2%)	1,075,000
Indefinite social distancing (SD)	42 mill (13.0%)	147,000
Relaxing social distancing		
SD relaxed May 1, 2020	269 mill (83.2%)	1,059,000
SD relaxed July 1, 2020	265 mill (82.0%)	1,039,000
SD relaxed September 1, 2020	263 mill (81.3%)	1,010,000

Table S1: Cumulative infections and deaths after 1 year for social distancing scenarios without testing.

S2. Model Equations

The ordinary differential equations describing the model are shown below for group i. The positive test group is denoted with the '+' sign.

$$
\begin{aligned}
\frac{dS_i}{dt} &= -\lambda_i(t)S_i - (1-sp)\times test_i(t)S_i \\
\frac{dE_i}{dt} &= \lambda_i(t)S_i - \gamma_e E_i - (1-sp)\times test_i(t)E_i \\
\frac{dI_{s,i}}{dt} &= \gamma_e E_i p - \gamma_s I_{s,i} \\
\frac{dI_{a,i}}{dt} &= \gamma_e E_i(1-p) - \gamma_a I_{a,i} - (1-sp)\times test_i(t)I_{a,i} \\
\frac{dH_{s,i}}{dt} &= \gamma_s I_{s,i}(Hosp_i - Crit_i) + \gamma_s I^+_{s,i}(Hosp_i - Crit_i) - \gamma_h H_{s,i} \\
\frac{dH_{c,i}}{dt} &= \gamma_s I_{s,i} Crit_i + \gamma_s I^+_{s,i} Crit_i - \gamma_h H_{c,i} \\
\frac{dD_i}{dt} &= \gamma_h H_{c,i} Die_i \\
\frac{dR_i}{dt} &= (1-Hosp_i)\gamma_s I_{s,i} + \gamma_a I_{a,i} + (1-se)\times m_2(t)\gamma_h H_{s,i} + (1-se)\times m_2(t)\gamma_h H_{c,i}(1-Die_i) \\
&\quad - se\times test_i(t)R_i + m_1(t)\gamma_h H_{s,i} + m_1(t)\gamma_h H_{c,i}(1-Die_i) \\
\frac{dS^+_i}{dt} &= (1-sp)test_i(t)S_i - \lambda^+_i(t)S^+_i \\
\frac{dE^+_i}{dt} &= (1-sp)test_i(t)E_i + \lambda^+_i(t)S^+_i - \gamma_e E^+_i \\
\frac{dI^+_{s,i}}{dt} &= \gamma_e E^+_i p - \gamma_s I^+_{s,i} \\
\frac{dI^+_{a,i}}{dt} &= (1-sp)\times test_i(t)I_{a,i} + \gamma_e E^+_i(1-p) - \gamma_a I^+_{a,i} \\
\frac{dR^+_i}{dt} &= se\times test_i(t)R_i + se\gamma_h m_2(t)H^+_{c,i}(1-Die_i) + \\
&\quad se\times m_2(t)\gamma_h H_{s,i} + (1-Hosp_i)\gamma_s I^+_{s,i} + \gamma_a I^+_{a,i}
\end{aligned}
$$

medRxiv preprint doi: https://doi.org/10.1101/2020.04.24.20078576; this version posted May 1, 2020. The copyright holder for this preprint (which was not certified by peer review) is the author/funder, who has granted medRxiv a license to display the preprint in perpetuity. It is made available under a CC-BY-NC-ND 4.0 International license .

$m_1(t)$ and $m_2(t)$ are defined as follows ($t = 107$ is when testing starts, on May 1, 2020):

$$m_1(t) = \{ \begin{array}{ll} 1 & t < 107 \\ 0 & t \geq 107 \end{array}$$

$$m_2(t) = \{ \begin{array}{ll} 0 & t < 107 \\ 1 & t \geq 107 \end{array}$$

The force of infection $\lambda(t)$ for the ith group is a function of the number of social contacts for age group i with each subgroup j at time t ($x_{i,j}(t)$), the probability of infection given contact (q), the number of infections in each group at time t ($infec_j(t)$), and the population size of each group at time t ($n_j(t)$). The overall equation for $\lambda_i(t)$ is shown below:

$$\lambda_i(t) = q\Bigg[\frac{x_{i,ch}(t)infect_{ch}(t)}{n_{ch}(t)} + \frac{x_{i,ch^+}(t)infect_{ch^+}(t)}{n_{ch^+}(t)} + \frac{x_{i,ad}(t)infect_{ad}(t)}{n_{ad}(t)}) + \frac{x_{i,ad^+}(t)infect_{ad^+}(t)}{n_{ad^+}(t)} + \frac{x_{i,rc}(t)infect_{rc}(t)}{n_{rc}(t)} + \frac{x_{i,rc^+}(t)infect_{rc^+}(t)}{n_{rc^+}(t)} + \frac{x_{i,fc}(t)infect_{fc}(t)}{n_{fc}(t)}) + \frac{x_{i,fc^+}(t)infect_{fc^+}(t)}{n_{fc^+}(t)} + \frac{x_{i,el}(t)infect_{el}(t)}{n_{el}(t)}) + \frac{x_{i,el^+}(t)infect_{el^+}(t)}{n_{el^+}(t)}\Bigg]$$

i and j take values of ch (children age 0-19 years), ad (adults age 20-65 years who are not working or working from home), el (older adults 65+ years of age), rc (adults at work in 'reduced-contact' occupations, where they have fewer contacts than pre-pandemic), fc (adults as work in full contact occupations, where they have the same number of contacts as pre-pandemic).

The number of infectious individuals by age group and test status is equal to the sum of documented (symptomatic) cases and a fraction of the undocumented (asymptomatic) cases, where this fraction asy corresponds to the relative infectiousness of undocumented cases. This is shown below for children:

$$infect_{ch}(t) = asyI_{a,c} + I_{s,c}$$

medRxiv preprint doi: https://doi.org/10.1101/2020.04.24.20078576; this version posted May 1, 2020. The copyright holder for this preprint (which was not certified by peer review) is the author/funder, who has granted medRxiv a license to display the preprint in perpetuity. It is made available under a CC-BY-NC-ND 4.0 International license .

S3. Model parameters

Parameters used in the model simulations are shown in Table S2. We assume that the size of the working population is stable over the duration of the simulation. Although this may not be the case as unemployment increases throughout the pandemic, the rate at which unemployment has increased so far has been time-varying and its future trajectory is unknown.

Where possible, parameters were taken from prior literature. However, data from the initial stages of the outbreak were lacking for the probability of death among ICU patients (Die_{ad} and Die_{el}) and the probability of transmission per contact (q). Several estimates of case fatality have been reported (including [28]), but these numbers have varied significantly by setting. As case fatality is often uncertain in the early stages of an epidemic, the value of $\mathcal{R}_0$ is better estimated using generation time data. Using this method, estimates of $\mathcal{R}_0$ have ranged between 2 and 3 [29]. We derived the expression for $\mathcal{R}_0$ based on our model and varied $\mathcal{R}_0$ within the credible range defined by previous studies. While we did not formally fit to incidence data, we tuned Die_{ad}, Die_{el}, and $\mathcal{R}_0$ to be consistent, within an order of magnitude, with reported death rates in early March 2020, before national social distancing began. We then calculated the resulting q value (see S4 for derivations of the basic reproduction number).

Based on this calibration, our model predicts 1.08 million deaths after one year, an infection fatality rate (IFR), of 0.4% and a case fatality rate (CFR) of 2.8% if no interventions were implemented (see Table S1). While our IFR estimates are lower than some other studies [28], we also assume a higher level of undocumented infections, which recent data suggest may considerably outnumber documented infections [6]. Our CFR estimates are similar to other studies.

It is important to note that the fraction of cases who are undocumented is presently uncertain, and overall results are highly sensitive to this quantity. For example, if we allow the fraction of cases that are documented to be 0.3, twice that reported by Li et al [6], our model predicts 2.4 million deaths, an IFR of 0.9%, and a CFR of 2.9%. This difference underscores the importance of collecting high quality serological data going forward.

Baseline social distancing parameters $sd.other$ and $p.reduced$ (when $c = 1$) were estimated by matching the observed peak time (at the beginning of April, around 100 days after the epidemic began) and incidence in early to mid-April, under national social distancing.

medRxiv preprint doi: https://doi.org/10.1101/2020.04.24.20078576; this version posted May 1, 2020. The copyright holder for this preprint (which was not certified by peer review) is the author/funder, who has granted medRxiv a license to display the preprint in perpetuity. It is made available under a CC-BY-NC-ND 4.0 International license .

Parameter	Code	Value	Units	Source(s)
Natural history				
Latent period	γ_e	1/3	1/days	[30]
Recovery rate, undocumented infections	γ_a	1/7	1/days	[22]
Recovery rate, documented infections	γ_s	1/7	1/days	[22]
Recovery rate, hospitalized cases	γ_h	1/15	1/days	[28]
Fraction undocumented	p	0.86	–	[6]
Relative infectiousness of undocumented infections	asy	0.55	–	[6]
Basic reproduction number	$\mathcal{R}_0$	2.9	–	estimated
Probability of infection per contact	q	0.0451	1/contact	estimated
Hospitalization				
Probability of hospitalization				
Children	$Hosp_{ch}$	0.061	–	[31]
Adults	$Hosp_{ad}$	0.182	–	[31]
Elderly	$Hosp_{el}$	0.417	–	[31]
Probability of requiring critical care				
Children	$Crit_{ch}$	0	–	[31]
Adults	$Critc_{ad}$	0.063	–	[31]
Elderly	$Crit_{el}$	0.173	–	[31]
Probability of death among critical care patients				
Children	Die_{ch}	0	–	[28]
Adults	Die_{ad}	0.5	–	estimated
Elderly	Die_{el}	0.5	–	estimated
Test features				
Sensitivity	se	0.94	–	[10]
Specificity	sp	0.96 (0.5, 1.0)	–	[10]
Population features				
Baseline contact rates by age	$x_{i,j}$	see matrices		[15]
US population age groups, size				[32]
Children		8.18e7	people	
Adults		18.7e7	people	
Elderly		5.89e7	people	
Adult working population segments, size				[33]
Exclusive work from home occupations	n_{home}	5.60e7	people	
Reduced contact occupations	$n_{reduced}$	1.20e8	people	
Full contact occupations	n_{full}	1.00e7	people	
Fraction of adult population (20-65 years) in workforce		1.0		assumption
Social distancing parameters				
Strength of social distancing	c	(0,1)	–	varied
Fraction of work contacts maintained for rc occupations	$p.reduced$	$1 - c0.90$	–	estimated
Fraction of 'other' contacts maintained for all groups	$sd.other$	$1 - c0.75$	–	estimated
Shielding	α	(0, 9)	per contact	varied
Testing rate		(0, 10 million)	per day	varied

Table S2: Parameters used in model simulations. Values shown in parentheses represent a range, used to perform sensitivity analysis.

medRxiv preprint doi: https://doi.org/10.1101/2020.04.24.20078576; this version posted May 1, 2020. The copyright holder for this preprint (which was not certified by peer review) is the author/funder, who has granted medRxiv a license to display the preprint in perpetuity. It is made available under a CC-BY-NC-ND 4.0 International license .

S4. Estimating transmission probability q using $\mathcal{R}_0$ Estimation

To estimate the transmission probability per infectious contact, q, we calculated the basic reproduction number for our model using the next generation method, substituted for other known model parameters, and solved for the value of q that satisfied a given value of $\mathcal{R}_0$. The dynamics of the system and $\mathcal{R}_0$ are determined by how the outbreak would proceed at time zero in the absence of any interventions. Therefore, we assume no testing at time 0, no social distancing, and no differences in worker contact levels (i.e., all groups mix at the population-average level prior to the outbreak). In this situation, there are only 3 population subgroups at time zero:

$$
\begin{aligned}
\frac{dE_{ch}}{dt} &= \lambda_{ch} S_{ch} - \gamma_e E_{ch} \\
\frac{dI_{s,ch}}{dt} &= \gamma_e E_{ch} p - \gamma_s I_{s,ch} \\
\frac{dI_{a,ch}}{dt} &= \gamma_e E_{ch}(1-p) - \gamma_a I_{a,ch} \\
\frac{dH_{s,ch}}{dt} &= \gamma_s I_{s,ch}(Hosp_{ch} - CritDie_{ch}) - \gamma_h Hosp_{s,ch} \\
\frac{dH_{c,ch}}{dt} &= \gamma_s I_{s,ch} CritDie_{ch} - \gamma_h Hosp_{c,ch} \\
\frac{dE_{ad}}{dt} &= \lambda_{ad} S_{ad} - \gamma_e E_{ad} \\
\frac{dI_{s,ad}}{dt} &= \gamma_e E_{ad} p - \gamma_s I_{s,ad} \\
\frac{dI_{a,ad}}{dt} &= \gamma_e E_{ad}(1-p) - \gamma_a I_{a,ad} \\
\frac{dH_{s,ad}}{dt} &= \gamma_s I_{s,ad}(Hosp_{ad} - CritDie_{ad}) - \gamma_h Hosp_{s,ad} \\
\frac{dH_{c,ad}}{dt} &= \gamma_s I_{s,ad} CritDie_{ad} - \gamma_h Hosp_{c,ad} \\
\frac{dE_{el}}{dt} &= \lambda_{el} S_{el} - \gamma_e E_{el} \\
\frac{dI_{s,el}}{dt} &= \gamma_e E_{el} p - \gamma_s I_{s,el} \\
\frac{dI_{a,el}}{dt} &= \gamma_e E_{el}(1-p) - \gamma_a I_{a,el} \\
\frac{dH_{s,el}}{dt} &= \gamma_s I_{s,el}(Hosp_{el} - CritDie_{el}) - \gamma_h Hosp_{s,el} \\
\frac{dH_{c,el}}{dt} &= \gamma_s I_{s,el} CritDie_{el} - \gamma_h Hosp_{c,el}
\end{aligned}
$$

The λ_i for each group is defined as follows.

$$
\lambda_{ch} = \frac{q x_{ch,ch}(asyI_{a,ch} + I_{s,ch})}{n_{ch}} + \frac{q x_{ch,ad}(asyI_{a,ad} + I_{s,ad})}{n_{ad}} + \frac{q x_{ch,el}(asyI_{a,el} + I_{s,el})}{n_{el}}
$$

medRxiv preprint doi: https://doi.org/10.1101/2020.04.24.20078576; this version posted May 1, 2020. The copyright holder for this preprint (which was not certified by peer review) is the author/funder, who has granted medRxiv a license to display the preprint in perpetuity. It is made available under a CC-BY-NC-ND 4.0 International license .

$$\lambda_{ad} = \frac{qx_{ad,ch}(asyI_{a,ch} + I_{s,ch})}{n_{ch}} + \frac{qx_{ad,ad}(asyI_{a,ad} + I_{s,ad})}{n_{ad}} + \frac{qx_{ad,el}(asyI_{a,el} + I_{s,el})}{n_{el}}$$

$$\lambda_{el} = \frac{qx_{el,ch}(asyI_{a,ch} + I_{s,ch})}{n_{ch}} + \frac{qx_{el,ad}(asyI_{a,ad} + I_{s,ad})}{n_{ad}} + \frac{qx_{el,el}(asyI_{a,el} + I_{s,el})}{n_{el}}$$

The matrices $\mathcal{F}$ and $\mathcal{V}$ corresponding to these equations are:

medRxiv preprint doi: https://doi.org/10.1101/2020.04.24.20078576; this version posted May 1, 2020. The copyright holder for this preprint **(which was not certified by peer review)** is the author/funder, who has granted medRxiv a license to display the preprint in perpetuity. It is made available under a CC-BY-NC-ND 4.0 International license .

$$\mathcal{F} = \begin{bmatrix}
0 & q^{x}_{ch,ch} & q^{x}_{ch,ch^{asy}} & 0 & 0 & q^{c}_{ch,ad} & q^{x}_{ch,ad^{asy}} & 0 & 0 & q^{x}_{ch,el} & q^{x}_{ch,el^{asy}} & 0 \\
0 & 0 & 0 & 0 & 0 & 0 & 0 & 0 & 0 & 0 & 0 & 0 \\
0 & 0 & 0 & 0 & 0 & 0 & 0 & 0 & 0 & 0 & 0 & 0 \\
0 & 0 & 0 & 0 & 0 & 0 & 0 & 0 & 0 & 0 & 0 & 0 \\
0 & 0 & 0 & 0 & 0 & 0 & 0 & 0 & 0 & 0 & 0 & 0 \\
0 & q^{x}_{ad,ch} & q^{x}_{ad,ch^{asy}} & 0 & 0 & q^{x}_{ad,ad} & q^{x}_{ad,ad^{asy}} & 0 & 0 & q^{x}_{ad,el} & q^{x}_{ad,el^{asy}} & 0 \\
0 & 0 & 0 & 0 & 0 & 0 & 0 & 0 & 0 & 0 & 0 & 0 \\
0 & 0 & 0 & 0 & 0 & 0 & 0 & 0 & 0 & 0 & 0 & 0 \\
0 & 0 & 0 & 0 & 0 & 0 & 0 & 0 & 0 & 0 & 0 & 0 \\
0 & q^{x}_{el,ch} & q^{x}_{el,ch^{asy}} & 0 & 0 & q^{x}_{el,ad} & q^{x}_{el,ad^{asy}} & 0 & 0 & q^{x}_{el,el} & q^{x}_{el,el^{asy}} & 0 \\
0 & 0 & 0 & 0 & 0 & 0 & 0 & 0 & 0 & 0 & 0 & 0 \\
0 & 0 & 0 & 0 & 0 & 0 & 0 & 0 & 0 & 0 & 0 & 0 \\
0 & 0 & 0 & 0 & 0 & 0 & 0 & 0 & 0 & 0 & 0 & 0
\end{bmatrix}$$

$$\mathcal{V} = \begin{bmatrix}
\gamma_e & 0 & 0 & 0 & 0 & 0 & 0 & 0 & 0 & 0 & 0 & 0 \\
-\gamma_e p & \gamma_s & 0 & 0 & 0 & 0 & 0 & 0 & 0 & 0 & 0 & 0 \\
-\gamma_e(1-p) & 0 & \gamma_a & 0 & 0 & 0 & 0 & 0 & 0 & 0 & 0 & 0 \\
0 & 0 & -\gamma_s(Hosp_{ch} - CritDie_{ch}) & \gamma_h & 0 & 0 & 0 & 0 & 0 & 0 & 0 & 0 \\
0 & 0 & -\gamma_s CritDie_{ch} & 0 & \gamma_h & 0 & 0 & 0 & 0 & 0 & 0 & 0 \\
0 & 0 & 0 & 0 & 0 & \gamma_e & 0 & 0 & 0 & 0 & 0 & 0 \\
0 & 0 & 0 & 0 & 0 & -\gamma_e p & \gamma_s & 0 & 0 & 0 & 0 & 0 \\
0 & 0 & 0 & 0 & 0 & -\gamma_e(1-p) & 0 & \gamma_a & 0 & 0 & 0 & 0 \\
0 & 0 & 0 & 0 & 0 & 0 & 0 & -\gamma_s(Hosp_{ad} - CritDie_{ad}) & \gamma_h & 0 & 0 & 0 \\
0 & 0 & 0 & 0 & 0 & 0 & 0 & -\gamma_s CritDie_{ad} & 0 & \gamma_h & 0 & 0 \\
0 & 0 & 0 & 0 & 0 & 0 & 0 & 0 & 0 & 0 & \gamma_e & 0 \\
0 & 0 & 0 & 0 & 0 & 0 & 0 & 0 & 0 & 0 & -\gamma_e p & \gamma_s \\
0 & 0 & 0 & 0 & 0 & 0 & 0 & 0 & 0 & 0 & -\gamma_e(1-p) & 0 \\
0 & 0 & 0 & 0 & 0 & 0 & 0 & 0 & 0 & 0 & 0

medRxiv preprint doi: https://doi.org/10.1101/2020.04.24.20078576; this version posted May 1, 2020. The copyright holder for this preprint (which was not certified by peer review) is the author/funder, who has granted medRxiv a license to display the preprint in perpetuity. It is made available under a CC-BY-NC-ND 4.0 International license .

To derive an expression for $\mathcal{R}_0$ we inverted the $\mathcal{V}$ matrix and multiplied by $\mathcal{F}$. The dominant eigenvalues of this matrix can be computed, but are very complex and are therefore not shown here. It is notable that because hospitalized cases do not contribute to the force of infection, the value of $\mathcal{R}_0$ does not depend on γ_h.

To estimate q, we fixed all other parameters to their initial values in the model. Then, $\mathcal{R}_0$ is given by $63.28q$. If $\mathcal{R}_0$ is 2.9 (the final value assumed in the model based on calibration with incidence data), that gives $q = 0.0451$.

S5. Contact matrices

Baseline contacts

Baseline contact matrices for 'work' contacts, 'school' contacts, 'home' contacts, and 'other' contacts were taken from [15]. To expand these baseline matrices to the 5 population groups in our model (separating the adult population into fc, rc, and h classes), we multiplied all contacts with adults $x_{i,ad}$ by the proportion of the adult population falling into each class. We define the fraction of the population falling in each working group as follows:

$$
\begin{aligned}
f.home &= \frac{n_{home}}{n_{home} + n_{reduced} + n_{full}} \\
f.reduced &= \frac{n_{reduced}}{n_{home} + n_{reduced} + n_{full}} \\
f.full &= \frac{n_{full}}{n_{home} + n_{reduced} + n_{full}}
\end{aligned}
$$

For baseline contact matrix values based on [15], we have:

$$
x_{i,j} = \begin{bmatrix} x_{ch,ch} & x_{ch,ad} & x_{ch,el} \\ x_{ad,ch} & x_{ad,ad} & x_{ad,el} \\ x_{el,ch} & x_{el,ad} & x_{el,el} \end{bmatrix}
$$

For simplicity, we assume that baseline interactions between worker subgroups are only assortative with respect to age (and not with respect to occupation type). To expand this matrix to a 5x5 matrix we use the following notation, where rows 2, 3, and 4 correspond to the work from home, reduced contact, and full contact occupation groups, respectively:

$$
x_{i,j} = \begin{bmatrix} x_{ch,ch} & x_{ch,ad}f.home & x_{ch,ad}f.reduced & x_{ch,ad}f.full & x_{ch,el} \\ x_{ad,ch} & x_{ad,ad}f.home & x_{ad,ad}f.reduced & x_{ad,ad}f.full & x_{ch,el} \\ x_{ad,ch} & x_{ad,ad}f.home & x_{ad,ad}f.reduced & x_{ad,ad}f.full & x_{ch,el} \\ x_{ad,ch} & x_{ad,ad}f.home & x_{ad,ad}f.reduced & x_{ad,ad}f.full & x_{ch,el} \\ x_{el,ch} & x_{el,ad}f.home & x_{el,ad}f.reduced & x_{el,ad}f.full & x_{ch,el} \end{bmatrix}
$$

medRxiv preprint doi: https://doi.org/10.1101/2020.04.24.20078576; this version posted May 1, 2020. The copyright holder for this preprint (which was not certified by peer review) is the author/funder, who has granted medRxiv a license to display the preprint in perpetuity. It is made available under a CC-BY-NC-ND 4.0 International license .

Based on these proportions, we define $x_{i,h}$, $x_{i,rc}$, and $x_{i,fc}$ as follows:

$$x_{i,h} = x_{i,ad} f.home$$
$$x_{i,rc} = x_{i,ad} f.reduced$$
$$x_{i,fc} = x_{i,ad} f.full$$

Contacts under social distancing

After social distancing has begun, we assume that:

- Home contacts remain the same.
- Schools and daycares close.
- Only working age adults continue to work. Baseline workplace contacts for children and young adults under 20 years of age are nearly zero (average 0.84 contacts/day) and the average workplace contacts for the elderly is 0, so this does not appreciably impact our results.
- All workers who are able work from home.
- Adults continuing to work reduce their workplace contacts by constant $preduced$.
- Other contacts are reduced by scalar constant $sd.other$.

The values of $p.reduced$ and $sd.other$ were estimated by comparing projected incidence from our model with that observed in the U.S. under social distancing measures.

The revised contact matrix for work contacts then becomes:

$$CM_{work} = \begin{bmatrix} 0 & 0 & 0 & 0 & 0 \\ 0 & 0 & 0 & 0 & 0 \\ x_{ad,ch} preduced & x_{h,h} p.reduced & x_{h,rc} p.reduced & x_{h,fc} p.reduced & x_{ch,el} preduced \\ x_{fc,ch} & x_{fc,h} & x_{fc,rc} & x_{fc,fc} & x_{ch,el} \\ 0 & 0 & 0 & 0 & 0 \end{bmatrix}$$

The revised contact matrix for other contacts becomes:

$$CM_{other} = sd.other \times \begin{bmatrix} x_{ch,ch} & x_{ch,h} & x_{ch,rc} & x_{ch,fc} & x_{ch,el} \\ x_{h,ch} & x_{h,h} & x_{h,rc} & x_{h,fc} & x_{ch,el} \\ x_{rc,ch} & x_{rc,h} & x_{rc,rc} & x_{rc,f} & x_{ch,el} \\ x_{fc,ch} & x_{fc,h} & x_{fc,rc} & x_{fc,fc} & x_{ch,el} \\ x_{el,ch} & x_{el,h} & x_{el,rc} & x_{el,fc} & x_{ch,el} \end{bmatrix}$$

medRxiv preprint doi: https://doi.org/10.1101/2020.04.24.20078576; this version posted May 1, 2020. The copyright holder for this preprint (which was not certified by peer review) is the author/funder, who has granted medRxiv a license to display the preprint in perpetuity. It is made available under a CC-BY-NC-ND 4.0 International license .

Contacts during initial relaxing of social distancing

When phase 1 begins on May 1, 2020, we assume that:

- Testing begins, moving test-positive individuals to the test positive group
- Home contacts remain the same, but their distribution is driven by the proportion of test-positives in the general population.
- Adults who were working from home may return to work if they test positive. Upon returning to work, their workplace contacts are assortative with respect to test status (but not with respect to occupation type).
- Workers in reduced contact occupations increase their workplace contacts based on the intensity of social distancing maintained. Work contacts are preferentially with test-positive individuals, as determined by α.
- Schools remain closed.
- Other contacts are increased for test positive individuals to their pre-pandemic levels. Other contacts continue to be reduced for test negative/untested individuals based on the intensity of social distancing maintained. Other contacts are preferentially with test-positive individuals, as determined by α.

Because testing has begun, all contact matrices are dependent on the proportion of the population that has tested positive and been released from social distancing at time t. We define this proportion as $r_i(t)$, where $(1 - r_i(t))$ is the fraction of the population who has not yet tested positive.

We assume that social distancing parameters are relaxed from their initial values as follows:

$$sd.other2 = 1 - (0.75c)$$
$$preduced = 1 - (0.90c)$$

For contact matrices of work and 'other' contacts, we implement shielding factor α, which increases the probability of contacting a test-positive individual according to their prevalence in the population (achieved by multiplying expected contact rates due to prevalence by scaling factor $\alpha + 1$). To account for the fact that, when prevalence is high, $(\alpha + 1)r_i(t)$ may exceed 1, we introduce a variable $s_i(t)$:

$$s_i(t) = \{ \begin{array}{cc} (\alpha+1)r_i(t) & (\alpha+1)r_i(t) \leq 1 \\ 1 & (\alpha+1)r_i(t) \geq 1 \end{array}$$

This shielding structure is similar to 'fixed shielding', previously described by Weitz et al [9] in that it preserves the baseline number of contacts and increases contacts for test positive individuals by $1 + \alpha$, as shown below:

medRxiv preprint doi: https://doi.org/10.1101/2020.04.24.20078576; this version posted May 1, 2020. The copyright holder for this preprint (which was not certified by peer review) is the author/funder, who has granted medRxiv a license to display the preprint in perpetuity. It is made available under a CC-BY-NC-ND 4.0 International license .

$$x_0 = x_0 r_i(t) + x_0(1 - r_i(t))$$
$$x_0 = r_i(t)(\alpha + 1)x_0 + (x_0 - (\alpha + 1)r_i(t)x_0)$$

The structure of all three matrices (home, work, and other) is given by CM:

medRxiv preprint doi: https://doi.org/10.1101/2020.04.24.20078576; this version posted May 1, 2020. The copyright holder for this preprint (which was not certified by peer review) is the author/funder, who has granted medRxiv a license to display the preprint in perpetuity. It is made available under a CC-BY-NC-ND 4.0 International license .

$$CM_{home} = \begin{bmatrix} r_{ch}(t)x_{ch,ch} & (1-r_{ch}(t))x_{ch,ch} & r_h(t)x_{ch,h} & (1-r_h(t))x_{ch,h} & r_{rc}(t)x_{ch,rc} & (1-r_{rc}(t))x_{ch,rc} & r_{fc}(t)x_{ch,fc} & (1-r_{fc}(t))x_{ch,fc} & r_{el}(t)x_{ch,el} & (1-r_{el}(t))x_{ch,el} \\ r_{ch}(t)x_{ch,ch} & (1-r_{ch}(t))x_{ch,ch} & r_h(t)x_{ch,h} & (1-r_h(t))x_{ch,h} & r_{rc}(t)x_{ch,rc} & (1-r_{rc}(t))x_{ch,rc} & r_{fc}(t)x_{ch,fc} & (1-r_{fc}(t))x_{ch,fc} & r_{el}(t)x_{ch,el} & (1-r_{el}(t))x_{ch,el} \\ r_{ch}(t)x_{h,ch} & (1-r_{ch}(t))x_{h,ch} & r_h(t)x_{h,h} & (1-r_h(t))x_{h,h} & r_{rc}(t)x_{h,rc} & (1-r_{rc}(t))x_{h,rc} & r_{fc}(t)x_{h,fc} & (1-r_{fc}(t))x_{h,fc} & r_{el}(t)x_{h,el} & (1-r_{el}(t))x_{h,el} \\ r_{ch}(t)x_{h,ch} & (1-r_{ch}(t))x_{h,ch} & r_h(t)x_{h,h} & (1-r_h(t))x_{h,h} & r_{rc}(t)x_{h,rc} & (1-r_{rc}(t))x_{h,rc} & r_{fc}(t)x_{h,fc} & (1-r_{fc}(t))x_{h,fc} & r_{el}(t)x_{h,el} & (1-r_{el}(t))x_{h,el} \\ r_{ch}(t)x_{rc,ch} & (1-r_{ch}(t))x_{rc,ch} & r_h(t)x_{rc,h} & (1-r_h(t))x_{rc,h} & r_{rc}(t)x_{rc,rc} & (1-r_{rc}(t))x_{rc,rc} & r_{fc}(t)x_{rc,fc} & (1-r_{fc}(t))x_{rc,fc} & r_{el}(t)x_{rc,el} & (1-r_{el}(t))x_{rc,el} \\ r_{ch}(t)x_{rc,ch} & (1-r_{ch}(t))x_{rc,ch} & r_h(t)x_{rc,h} & (1-r_h(t))x_{rc,h} & r_{rc}(t)x_{rc,rc} & (1-r_{rc}(t))x_{rc,rc} & r_{fc}(t)x_{rc,fc} & (1-r_{fc}(t))x_{rc,fc} & r_{el}(t)x_{rc,el} & (1-r_{el}(t))x_{rc,el} \end{bmatrix}$$

$$CM_{other} = \begin{bmatrix} 1 \\ sd.other2 \\ 1 \\ sd.other2 \\ 1 \\ sd.other2 \\ 1 \\ sd.other2 \\ 1 \\ sd.other2 \end{bmatrix} \times \begin{bmatrix} s_{ch}(t)x_{ch,ch} & (1-s_{ch}(t))x_{ch,ch} & s_h(t)x_{ch,h} & (1-s_h(t))x_{ch,h} & s_{rc}(t)x_{ch,rc} & (1-s_{rc}(t))x_{ch,rc} & s_{fc}(t)x_{ch,fc} & (1-s_{fc}(t))x_{ch,fc} & s_{el}(t)x_{ch,el} & (1-s_{el}(t))x_{ch,el} \\ s_{ch}(t)x_{ch,ch} & (1-s_{ch}(t))x_{ch,ch} & s_h(t)x_{ch,h} & (1-s_h(t))x_{ch,h} & s_{rc}(t)x_{ch,rc} & (1-s_{rc}(t))x_{ch,rc} & s_{fc}(t)x_{ch,fc} & (1-s_{fc}(t))x_{ch,fc} & s_{el}(t)x_{ch,el} & (1-s_{el}(t))x_{ch,el} \\ s_{ch}(t)x_{h,ch} & (1-s_{ch}(t))x_{h,ch} & s_h(t)x_{h,h} & (1-s_h(t))x_{h,h} & s_{rc}(t)x_{h,rc} & (1-s_{rc}(t))x_{h,rc} & s_{fc}(t)x_{h,fc} & (1-s_{fc}(t))x_{h,fc} & s_{el}(t)x_{h,el} & (1-s_{el}(t))x_{h,el} \\ s_{ch}(t)x_{h,ch} & (1-s_{ch}(t))x_{h,ch} & s_h(t)x_{h,h} & (1-s_h(t))x_{h,h} & s_{rc}(t)x_{h,rc} & (1-s_{rc}(t))x_{h,rc} & s_{fc}(t)x_{h,fc} & (1-s_{fc}(t))x_{h,fc} & s_{el}(t)x_{h,el} & (1-s_{el}(t))x_{h,el} \\ s_{ch}(t)x_{rc,ch} & (1-s_{ch}(t))x_{rc,ch} & s_h(t)x_{rc,h} & (1-s_h(t))x_{rc,h} & s_{rc}(t)x_{rc,rc} & (1-s_{rc}(t))x_{rc,rc} & s_{fc}(t)x_{rc,fc} & (1-s_{fc}(t))x_{rc,fc} & s_{el}(t)x_{rc,el} & (1-s_{el}(t))x_{rc,el} \\ s_{ch}(t)x_{rc,ch} & (1-s_{ch}(t))x_{rc,ch} & s_h(t)x_{rc,h} & (1-s_h(t))x_{rc,h} & s_{rc}(t)x_{rc,rc} & (1-s_{rc}(t))x_{rc,rc} & s_{fc}(t)x_{rc,fc} & (1-s_{fc}(t))x_{rc,fc} & s_{el}(t)x_{rc,el} & (1-s_{el}(t))x_{rc,el} \\ s_{ch}(t)x_{fc,ch} & (1-s_{ch}(t))x_{fc,ch} & s_h(t)x_{fc,h} & (1-s_h(t))x_{fc,h} & s_{rc}(t)x_{fc,rc} & (1-s_{rc}(t))x_{fc,rc} & s_{fc}(t)x_{fc,fc} & (1-s_{fc}(t))x_{fc,fc} & s_{el}(t)x_{fc,el} & (1-s_{el}(t))x_{fc,el} \\ s_{ch}(t)x_{fc,ch} & (1-s_{ch}(t))x_{fc,ch} & s_h(t)x_{fc,h} & (1-s_h(t))x_{fc,h} & s_{rc}(t)x_{fc,rc} & (1-s_{rc}(t))x_{fc,rc} & s_{fc}(t)x_{fc,fc} & (1-s_{fc}(t))x_{fc,fc} & s_{el}(t)x_{fc,el} & (1-s_{el}(t))x_{fc,el} \\ s_{ch}(t)x_{el,ch} & (1-s_{ch}(t))x_{el,ch} & s_h(t)x_{el,h} & (1-s_h(t))x_{el,h} & s_{rc}(t)x_{el,rc} & (1-s_{rc}(t))x_{el,rc} & s_{fc}(t)x_{el,fc} & (1-s_{fc}(t))x_{el,fc} & s_{el}(t)x_{el,el} & (1-s_{el}(t))x_{el,el} \\ s_{ch}(t)x_{el,ch} & (1-s_{ch}(t))x_{el,ch} & s_h(t)x_{el,h} & (1-s_h(t))x_{el,h} & s_{rc}(t)x_{el,rc} & (1-s_{rc}(t))x_{el,rc} & s_{fc}(t)x_{el,fc} & (1-s_{fc}(t))x_{el,fc} & s_{el}(t)x_{el,el} & (1-s_{el}(t))x_{el,el} \end{bmatrix}$$

$$CM_{work} = \begin{bmatrix} 0 \\ 0 \\ 1 \\ 0 \\ preduced2 \\ preduced2 \\ 1 \\ 1 \\ 0 \\ 0 \end{bmatrix} \times \begin{bmatrix} 0 & 0 & 0 & 0 & 0 & 0 & 0 & 0 & 0 & 0 \\ 0 & 0 & 0 & 0 & 0 & 0 & 0 & 0 & 0 & 0 \\ x_{h,ch} & 0 & x_{h,h} & 0 & x_{h,rc} & 0 & x_{h,fc} & 0 & x_{h,el} & 0 \\ 0 & 0 & 0 & 0 & 0 & 0 & 0 & 0 & 0 & 0 \\ s_{ch}(t)x_{rc,ch} & (1-s_{ch}(t))x_{rc,ch} & s_h(t)x_{rc,h} & (1-s_h(t))x_{rc,h} & s_{rc}(t)x_{rc,rc} & (1-s_{rc}(t))x_{rc,rc} & s_{fc}(t)x_{rc,fc} & (1-s_{fc}(t))x_{rc,fc} & s_{el}(t)x_{rc,el} & (1-s_{el}(t))x_{rc,el} \\ s_{ch}(t)x_{rc,ch} & (1-s_{ch}(t))x_{rc,ch} & s_h(t)x_{rc,h} & (1-s_h(t))x_{rc,h} & s_{rc}(t)x_{rc,rc} & (1-s_{rc}(t))x_{rc,rc} & s_{fc}(t)x_{rc,fc} & (1-s_{fc}(t))x_{rc,fc} & s_{el}(t)x_{rc,el} & (1-s_{el}(t))x_{rc,el} \\ 0 & 0 & 0 & 0 & 0 & 0 & 0 & 0 & 0 & 0 \\ 0 & 0 & 0 & 0 & 0 & 0 & 0 & 0 & 0 & 0 \end{bmatrix}$$

medRxiv preprint doi: https://doi.org/10.1101/2020.04.24.20078576; this version posted May 1, 2020. The copyright holder for this preprint (which was not certified by peer review) is the author/funder, who has granted medRxiv a license to display the preprint in perpetuity. It is made available under a CC-BY-NC-ND 4.0 International license .

Contacts after schools reopen on September 1, 2020

When phase 2 begins, schools re-open and children return to school, setting the school contact matrix to its baseline values. Because some children will have tested positive, contact probabilities are proportional to the fraction of the population who has tested positive at each time point (same structure as the home matrix from phase 1). All other matrices remain the same.

S6. Contact reductions by levels of c

c	Reduction in work contacts for adults	Reduction in other contacts for all groups	Reduction in total contacts		
			Children	Adults	Elderly
0	0%	0%	38.9%	17.9%	33.7%
0.25	45.7%	18.8%	44.9%	29.5%	44.2%
0.50	59.8%	37.5%	51.0%	41.2%	54.6%
0.75	73.9%	56.3%	57.1%	53.0%	65.1%
1.00	88.1%	75.0%	63.1%	64.7%	75.5%

Table S3: Reduction in contacts corresponding to different values of c

S7. Test performance over time

While not all test positive individuals are truly immune, the proportion of immune persons is always far greater in the test-positive population than the test-negative/untested population. Thus, even though the positive predictive value for a test does not approach 100% as the epidemic proceeds and a substantial number of truly susceptible individuals are identified as positive, preferential interaction with test-positive individuals tends to decrease risk. Higher testing rates tend to lead to lower immunity in the test positive population because a greater number of false positives are released from social distancing, and when shielding is strong these test positives mix to a greater extent with the test-negative/untested population, contributing to ongoing transmission. The level of immunity in the test positive population is shown in FigureS2 below for 5:1 shielding. Overall immunity is higher in the test-positive population (e.g., fewer false positives) when alpha is smaller (not shown).

medRxiv preprint doi: https://doi.org/10.1101/2020.04.24.20078576; this version posted May 1, 2020. The copyright holder for this preprint (which was not certified by peer review) is the author/funder, who has granted medRxiv a license to display the preprint in perpetuity. It is made available under a CC-BY-NC-ND 4.0 International license .

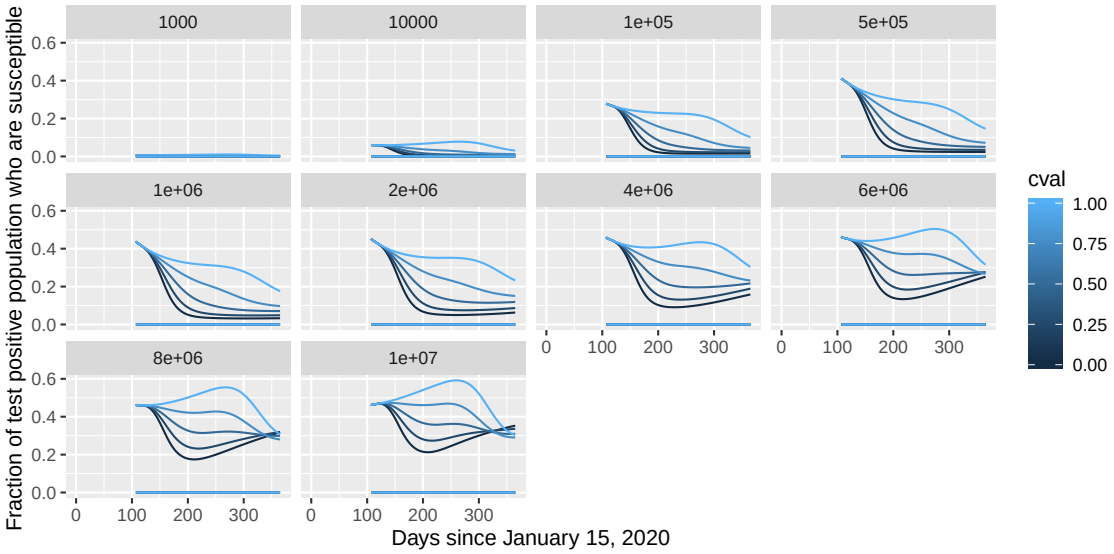

Figure S2: Fraction of test positives who are still susceptible to COVID-19 over time based on the testing rate (panels) and the intensity of social distancing (line colors) for 5:1 shielding ($\alpha = 4$).

S8. Sensitivity analysis for higher levels of shielding ($\alpha = 9$, 10:1 shielding)

We also considered higher levels of shielding to see how this change would impact cumulative deaths and the fraction of the population released from social distancing. While 10:1 shielding did result in fewer deaths at high testing levels, the total impact was minimal (Figure S3).

medRxiv preprint doi: https://doi.org/10.1101/2020.04.24.20078576; this version posted May 1, 2020. The copyright holder for this preprint (which was not certified by peer review) is the author/funder, who has granted medRxiv a license to display the preprint in perpetuity. It is made available under a CC-BY-NC-ND 4.0 International license .

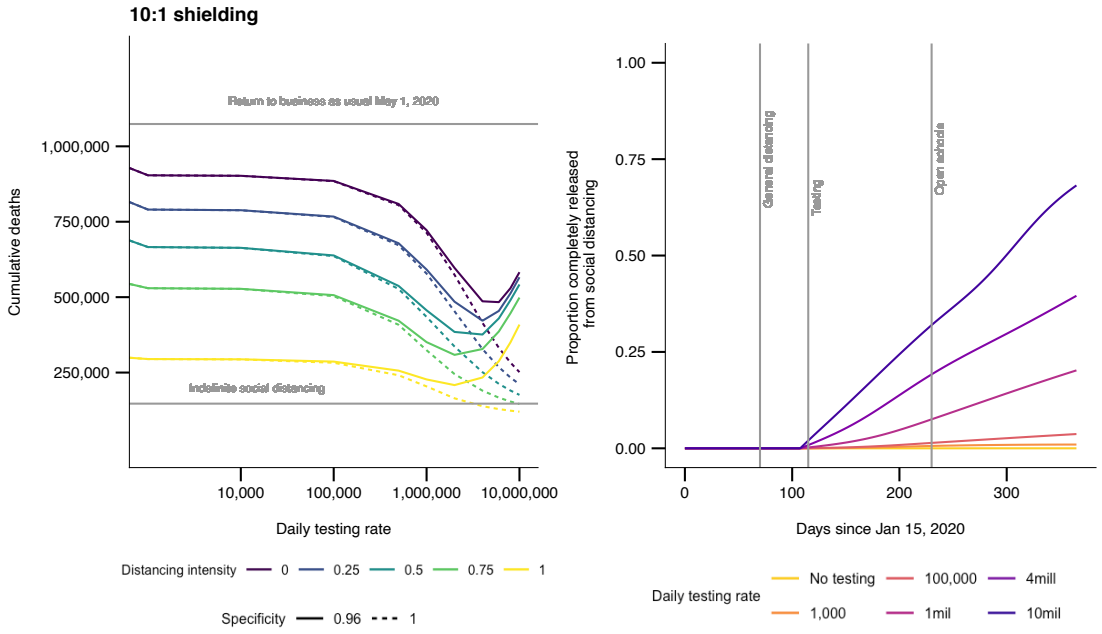

Figure S3: The left panel shows cumulative deaths by January 15, 2021 by social distancing relaxing strategy assuming schools reopen on September 1, 2020. Colored lines show levels of relaxing social distancing measures based on the value of c. Solid lines are for 96% specificity and dashed lines show results for a test with 100% specificity. The right panel shows the fraction of the US population released from social distancing after 1 year assuming a 50% relaxation of current social distancing levels or work and other contacts for those untested or testing negative and a 96% test specificity. Line colors correspond to testing levels, with blue being 10 million tests/day (monthly testing of the US population). Both panels are for 10:1 Shielding ($\alpha = 9$).

medRxiv preprint doi: https://doi.org/10.1101/2020.04.24.20078576; this version posted May 1, 2020. The copyright holder for this preprint (which was not certified by peer review) is the author/funder, who has granted medRxiv a license to display the preprint in perpetuity. It is made available under a CC-BY-NC-ND 4.0 International license .

S9. Sensitivity analysis for varying specificity

If antibodies do not confer immunity against subsequent infection (approximated by setting $sp = 0.5$), increased testing leads to higher rates of death (Figure S4).

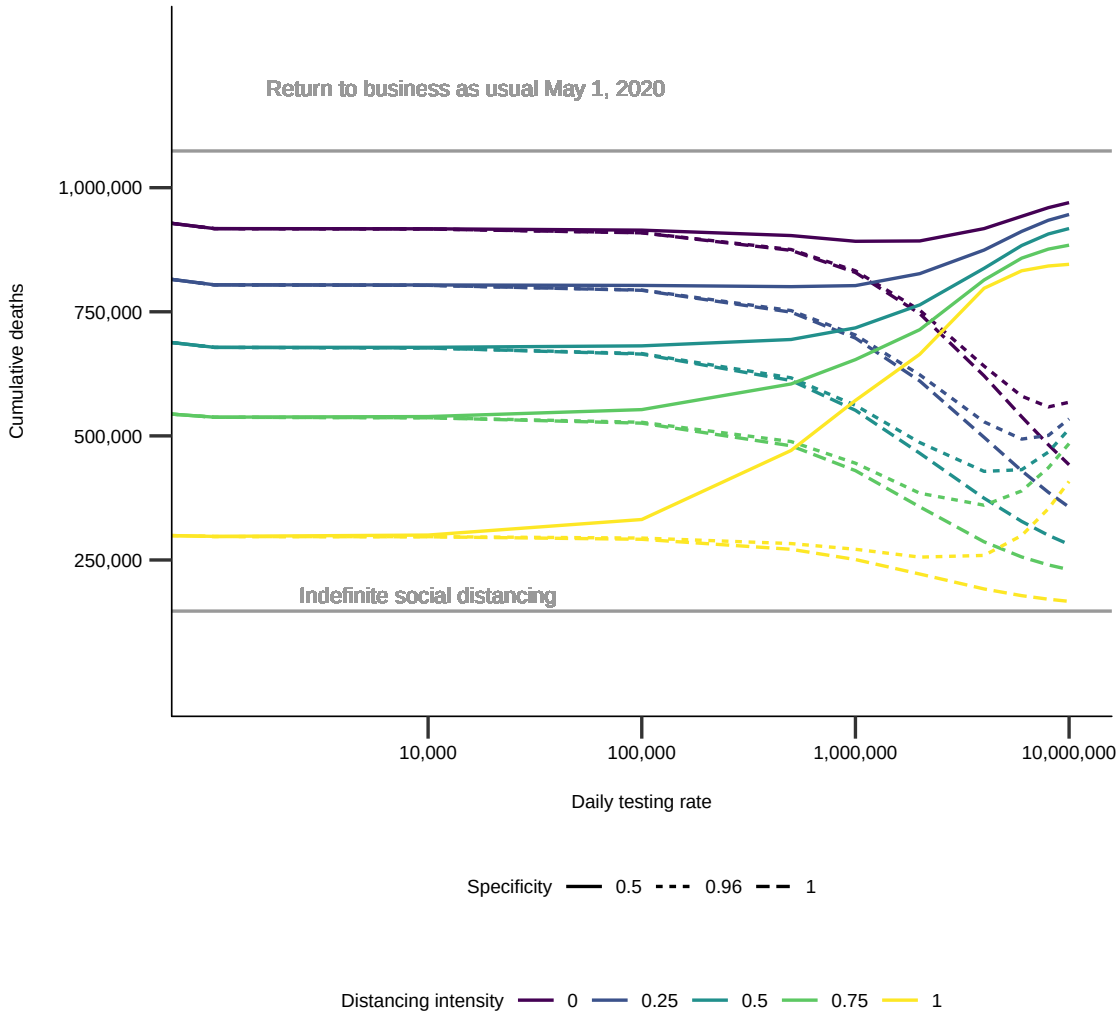

Figure S4: Deaths after 1 year assuming $\alpha = 4$ (5:1 shielding) and $sp = 0.50$ (solid line) or $sp = 0.96$ (dotted line), or $sp = 1.00$ (dashed line)

References

[1] COVID-19 Map;. Library Catalog: coronavirus.jhu.edu. Available from: `https://coronavirus.jhu.edu/map.html`.

[2] Woodward HS Aylin. About 95% of Americans have been ordered to stay at home. This map shows which cities and states are under lockdown.;. Library Catalog: www.businessinsider.com. Available from: `https://www.businessinsider.com/us-map-stay-at-home-orders-lockdowns-2020-3`.

medRxiv preprint doi: https://doi.org/10.1101/2020.04.24.20078576; this version posted May 1, 2020. The copyright holder for this preprint (which was not certified by peer review) is the author/funder, who has granted medRxiv a license to display the preprint in perpetuity. It is made available under a CC-BY-NC-ND 4.0 International license .

[3] McFall-Johnsen MJK Lauren Frias. A third of the global population is on coronavirus lockdown — here's our constantly updated list of countries and restrictions;. Available from: https://www.businessinsider.com/countries-on-lockdown-coronavirus-italy-2020-3.

[4] National coronavirus response: A road map to reopening;. Library Catalog: www.aei.org Section: Health Policy. Available from: https://www.aei.org/research-products/report/national-coronavirus-response-a-road-map-to-reopening/.

[5] Ferguson N. Report 9: Impact of non-pharmaceutical interventions (NPIs) to reduce COVID-19 mortality and healthcare demand;. Available from: https://www.imperial.ac.uk/media/imperial-college/medicine/sph/ide/gida-fellowships/Imperial-College-COVID19-NPI-modelling-16-03-2020.pdf.

[6] Li R, Pei S, Chen B, Song Y, Zhang T, Yang W, et al. Substantial undocumented infection facilitates the rapid dissemination of novel coronavirus (SARS-CoV2). Science. 2020 Mar;p. eabb3221. Available from: https://www.sciencemag.org/lookup/doi/10.1126/science.abb3221.

[7] Cutts FT, Hanson M. Seroepidemiology: an underused tool for designing and monitoring vaccination programmes in low- and middle-income countries. Tropical Medicine & International Health. 2016;21(9):1086–1098. Available from: https://onlinelibrary.wiley.com/doi/abs/10.1111/tmi.12737.

[8] Coronavirus: Germany plans COVID-19 'immunity certificates' testing - Business Insider;. Available from: https://www.businessinsider.com/coronavirus-germany-covid-19-immunity-certificates-testing-social-distancing-lockdown-2020-3?r=US&IR=T.

[9] Weitz JS, Beckett SJ, Coenen AR, Demory D, Dominguez-Mirazo M, Dushoff J, et al. Intervention Serology and Interaction Substitution: Modeling the Role of 'Shield Immunity' in Reducing COVID-19 Epidemic Spread. medRxiv. 2020 Apr;p. 2020.04.01.20049767. Available from: https://www.medrxiv.org/content/10.1101/2020.04.01.20049767v1.

[10] qSARS-CoV-2 IgG/IgM Rapid Test;. Available from: https://www.fda.gov/media/136622/download.

[11] Emory develops diagnostic antibody blood test to determine antibody-responses to COVID-19; 2020. Available from: https://news.emory.edu/stories/2020/04/coronavirus_antibody_blood_test/index.html.

[12] Adams ER, Anand R, Andersson MI, Auckland K, Baillie JK, Barnes E, et al. Evaluation of antibody testing for SARS-Cov-2 using ELISA and lateral flow immunoassays. medRxiv. 2020 Apr;p. 2020.04.15.20066407. Publisher: Cold Spring Harbor Laboratory Press. Available from: https://www.medrxiv.org/content/10.1101/2020.04.15.20066407v1.

[13] Lassaunière R, Frische A, Harboe ZB, Nielsen AC, Fomsgaard A, Krogfelt KA, et al. Evaluation of nine commercial SARS-CoV-2 immunoassays. medRxiv. 2020 Apr;p. 2020.04.09.20056325. Publisher: Cold Spring Harbor Laboratory Press. Available from: https://www.medrxiv.org/content/10.1101/2020.04.09.20056325v1.

medRxiv preprint doi: https://doi.org/10.1101/2020.04.24.20078576; this version posted May 1, 2020. The copyright holder for this preprint (which was not certified by peer review) is the author/funder, who has granted medRxiv a license to display the preprint in perpetuity. It is made available under a CC-BY-NC-ND 4.0 International license .

[14] Mossong J, Hens N, Jit M, Beutels P, Auranen K, Mikolajczyk R, et al. Social Contacts and Mixing Patterns Relevant to the Spread of Infectious Diseases. PLOS Medicine. 2008 Mar;5(3):e74. Available from: https://journals.plos.org/plosmedicine/article?id=10.1371/journal.pmed.0050074.

[15] Prem K, Cook AR, Jit M. Projecting social contact matrices in 152 countries using contact surveys and demographic data. PLOS Computational Biology. 2017 Sep;13(9):e1005697. Publisher: Public Library of Science. Available from: https://journals.plos.org/ploscompbiol/article?id=10.1371/journal.pcbi.1005697.

[16] Cryptic transmission of novel coronavirus revealed by genomic epidemiology;. Available from: https://bedford.io/blog/ncov-cryptic-transmission/.

[17] Holshue ML, DeBolt C, Lindquist S, Lofy KH, Wiesman J, Bruce H, et al. First Case of 2019 Novel Coronavirus in the United States. New England Journal of Medicine. 2020 Mar;382(10):929–936. Available from: http://www.nejm.org/doi/10.1056/NEJMoa2001191.

[18] Remarks by President Trump, Vice President Pence, and Members of the Coronavirus Task Force in Press Briefing;. Available from: https://www.whitehouse.gov/briefings-statements/remarks-president-trump-vice-president-pence-members-coronavirus-task-force-press-briefing-4/.

[19] Quantifying interpersonal contact in the United States during the spread of COVID-19: first results from the Berkeley Interpersonal Contact Study | medRxiv;. Available from: https://www.medrxiv.org/content/10.1101/2020.04.13.20064014v1.

[20] Fast Facts on U.S. Hospitals, 2020 | AHA;. Library Catalog: www.aha.org. Available from: https://www.aha.org/statistics/fast-facts-us-hospitals.

[21] Chan KH, Peiris JSM, Lam SY, Poon LLM, Yuen KY, Seto WH. The Effects of Temperature and Relative Humidity on the Viability of the SARS Coronavirus [Research Article]; 2011. ISSN: 1687-8639 Library Catalog: www.hindawi.com Pages: e734690 Publisher: Hindawi Volume: 2011. Available from: https://www.hindawi.com/journals/av/2011/734690/.

[22] Kissler SM, Tedijanto C, Goldstein E, Grad YH, Lipsitch M. Projecting the transmission dynamics of SARS-CoV-2 through the postpandemic period. Science. 2020 Apr;Publisher: American Association for the Advancement of Science Section: Report. Available from: https://science.sciencemag.org/content/early/2020/04/14/science.abb5793.

[23] Bennhold K, Vancon L. With Broad, Random Tests for Antibodies, Germany Seeks Path Out of Lockdown. The New York Times. 2020 Apr;Available from: https://www.nytimes.com/2020/04/18/world/europe/with-broad-random-tests-for-antibodies-germany-seeks-path-out-of-lockdown.html.

[24] Peeri NC, Shrestha N, Rahman MS, Zaki R, Tan Z, Bibi S, et al. The SARS, MERS and novel coronavirus (COVID-19) epidemics, the newest and biggest global health threats: what lessons have we learned? International Journal of Epidemiology;Available from: https://academic.oup.com/ije/article/doi/10.1093/ije/dyaa033/5748175.

[25] Gray N, Calleja D, Wimbush A, Miralles-Dolz E, Gray A, De-Angelis M, et al. ”No test is better than a bad test”: Impact of diagnostic uncertainty in mass testing on the spread of Covid-19. medRxiv.

medRxiv preprint doi: https://doi.org/10.1101/2020.04.24.20078576; this version posted May 1, 2020. The copyright holder for this preprint (which was not certified by peer review) is the author/funder, who has granted medRxiv a license to display the preprint in perpetuity. It is made available under a CC-BY-NC-ND 4.0 International license .

2020 Apr;p. 2020.04.16.20067884. Publisher: Cold Spring Harbor Laboratory Press. Available from: https://www.medrxiv.org/content/10.1101/2020.04.16.20067884v1.

[26] Zhao J, Yuan Q, Wang H, Liu W, Liao X, Su Y, et al. Antibody responses to SARS-CoV-2 in patients of novel coronavirus disease 2019. Clinical Infectious Diseases;Available from: https://academic.oup.com/cid/article/doi/10.1093/cid/ciaa344/5812996.

[27] Huang AT, Garcia-Carreras B, Hitchings MDT, Yang B, Katzelnick L, Rattigan SM, et al. A systematic review of antibody mediated immunity to coronaviruses: antibody kinetics, correlates of protection, and association of antibody responses with severity of disease. Infectious Diseases (except HIV/AIDS); 2020. Available from: http://medrxiv.org/lookup/doi/10.1101/2020.04.14.20065771.

[28] Zhou F, Yu T, Du R, Fan G, Liu Y, Liu Z, et al. Clinical course and risk factors for mortality of adult inpatients with COVID-19 in Wuhan, China: a retrospective cohort study. The Lancet. 2020 Mar;395(10229):1054–1062. Publisher: Elsevier. Available from: https://www.thelancet.com/journals/lancet/article/PIIS0140-6736(20)30566-3/abstract.

[29] Liu Y, Gayle AA, Wilder-Smith A, Rocklöv J. The reproductive number of COVID-19 is higher compared to SARS coronavirus. Journal of Travel Medicine. 2020 Mar;27(2). Publisher: Oxford Academic. Available from: https://academic.oup.com/jtm/article/27/2/taaa021/5735319.

[30] He X, Lau EHY, Wu P, Deng X, Wang J, Hao X, et al. Temporal dynamics in viral shedding and transmissibility of COVID-19. Nature Medicine. 2020 Apr;p. 1–4. Publisher: Nature Publishing Group. Available from: https://www.nature.com/articles/s41591-020-0869-5.

[31] CDCMMWR. Severe Outcomes Among Patients with Coronavirus Disease 2019 (COVID-19) — United States, February 12–March 16, 2020. MMWR Morbidity and Mortality Weekly Report. 2020;69. Available from: https://www.cdc.gov/mmwr/volumes/69/wr/mm6912e2.htm.

[32] Bureau UC. Age and Sex Composition in the United States: 2018;. Available from: https://www.census.gov/data/tables/2018/demo/age-and-sex/2018-age-sex-composition.html.

[33] May 2019 OES National Industry-Specific Occupational Employment and Wage Estimates;. Library Catalog: www.bls.gov. Available from: https://www.bls.gov/oes/current/oessrci.htm.